Thermochimica Acta, 181 (1991) 253–268
Elsevier Science Publishers B.V., Amsterdam

THERMAL DECOMPOSITION KINETICS. PART XVII. KINETICS AND MECHANISM OF THERMAL DECOMPOSITION OF BIS(ETHYLENEDIAMINE)COPPER(II) HALIDE MONOHYDRATE

SURESH MATHEW and C.G.R. NAIR

Department of Chemistry, University of Kerala, Trivandrum 695 034 (India)

K.N. NINAN

Propellants and Special Chemicals Group, Vikram Sarabhai Space Centre, Trivandrum 695 022 (India)

(Received 14 September 1990)

ABSTRACT

The thermal decomposition studies of bis(ethylenediamine)copper(II) chloride monohydrate and bis(ethylenediamine)copper(II) bromide monohydrate were carried out using thermogravimetry (TG), derivative thermogravimetry (DTG) and differential thermal analysis (DTA). The kinetics and mechanism of the dehydration and the deamination stages of both the complexes were evaluated. The different stages of decomposition were identified from TG, DTG and DTA. The intermediate and residue analysis done using optical microscopy and X-ray diffraction showed the formation of CuCl and CuBr at about 450 °C and copper as fine linear wires at about 700 °C. The kinetic parameters for the dehydration and the deamination reactions were evaluated from the TG and DTA curves using four integral methods. For both the complexes the dehydration and the deamination processes follow the mechanism of random nucleation with the formation of one nucleus on each particle (Mampel equation). The heat of reaction for each stage of decomposition was determined using DTA.

INTRODUCTION

Recently, increasing interest has been bestowed on the thermal decomposition of transition metal ammine complexes in the solid state [1–4]. Both isothermal and non-isothermal methods have been used to evaluate the kinetics and mechanism of thermal decomposition reactions. A search through the literature revealed that very few attempts have been made to undertake a quantitative study on the kinetics and mechanism of their thermal deamination and dehydration reactions.

In preceding papers of this series, we reported the kinetic and mechanistic aspects of thermal decomposition of complexes containing both monoden-

0040-6031/91/$03.50

tate and bidentate ligands [5,6]. The present study investigates the kinetic, mechanistic and thermodynamic aspects of the thermal decomposition of ammine complexes of copper(II) containing halogen as the counter-anion in the solid phase using non-isothermal TG, DTG, DTA and other accessory techniques.

EXPERIMENTAL

Preparation of complexes

The complexes $[Cu(en)_2]Cl_2 \cdot H_2O$ and $[Cu(en)_2]Br_2 \cdot H_2O$ were prepared according to the procedure described in the literature, with slight modification [7]. A stoichiometric amount of ethylenediamine was added to an ethanolic solution of the corresponding metallic halide with stirring, and the solution was cooled in crushed ice. The complexes were precipitated by the addition of acetone with stirring. The isolated complexes were washed with acetone and then dried in vacuo over phosphorus(V) oxide. The resulting pink coloured complexes were characterized by spectral and chemical methods. The copper content in the complexes was analysed gravimetrically. Elemental analysis was carried out using a Carlo Erba microelemental analyser. Chlorine and bromine were estimated by the Volhard method. The results of the analysis are shown in Table 1.

Instruments

The TG, DTG and DTA curves were recorded using a DuPont model 2000 Thermal Analyst in conjunction with a 951 thermogravimetric analyser and 1200 DTA cell. The experiments were carried out in a pure nitrogen atmosphere at a flow rate of 50 cm^3 min^{-1}. The heating rate employed was 10 °C min^{-1} and the sample mass was 8.5 mg. The area under the DTA curves was evaluated by sigmoidal curve integration using the Thermal

TABLE 1

Analytical results for copper(II) halide complexes

	$[Cu(en)_2]Cl_2 \cdot H_2O$		$[Cu(en)_2]Br_2 \cdot H_2O$	
	Theoretical	Observed	Theoretical	Observed
Copper	23.32	23.94	17.58	17.75
Carbon	17.61	17.84	13.28	13.04
Hydrogen	6.60	6.73	4.98	4.89
Nitrogen	20.55	20.23	15.49	14.98
Chlorine	26.02	25.80		
Bromine			44.22	43.84

Analysis Software and calibration was done using pure indium and lead in the appropriate temperature ranges for enthalpy measurements. The X-ray powder diffractograms were recorded using a Philips 1710 diffractometer with a PW1729 X-ray generator using Cu $K\alpha$ radiation. Computational work was done with an IBM-PC/XT machine using the FORTRAN 77 program.

Mathematical treatment of data

Kinetic parameters were calculated from the TG–DTA curves using four non-mechanistic methods. The forms of these equations used are given below wherein the integral form of $g(\alpha)$ has been introduced for convenience and is defined as

$$g(\alpha) = \frac{1-(1-\alpha)^{1-n}}{1-n}$$

where α is the fractional decomposition at time t related to the sample mass from TG as m_t/m_∞ and DTA area as A_t/A_∞ (∞ refers to completion of reaction) and n is an order parameter.

Coats–Redfern equation [8]:

$$\ln[g(\alpha)/T^2] = \ln[AR/\phi E(1-2RT/E)] - E/RT$$

MacCallum–Tanner equation [9]:

$$\log_{10} g(\alpha) = \log_{10}[AE/\phi R] - 0.485E^{0.435} - \frac{[0.449+0.217E]\times 10^9}{T}$$

Horowitz–Metzger equation [10]:

$$\ln\, g(\alpha) = \ln[ART_s^2/\phi E] - E/RT_s + E\theta/RT_s^2$$

MKN equation [11]:

$$\ln[g(\alpha)/T^{1.9215}] = \ln[AE/\phi R] + 3.7721 - 1.9215 \ln E - 0.12039(E/T)$$

where T is the temperature (K), A is the pre-exponential factor, ϕ is the heating rate (°C min^{-1}), E is the energy of activation, R is the gas constant, T_s is the DTG/DTA peak temperature, and $\theta = T - T_s$.

Evaluation of kinetic and thermodynamic parameters

The order parameters were evaluated by an iteration method using the Coats–Redfern equation. Using a computer, linear plots of $\ln[g(\alpha)/T^2]$ vs. the reciprocal of the absolute temperature ($1/T$) were drawn by the method of least squares, taking the α and the corresponding T values from the TG curve. Linear curves were drawn for different values of n ranging from 0 to 2, in increments of 0.01. The value of n which gave the best fit was chosen as the order parameter.

The kinetic parameters were calculated from the linear plots of the left-hand side of the kinetic equations against $1/T$ for all the equations except the Horowitz–Metzger equation, for which the left-hand side is plotted against θ. The values of E and A were calculated, respectively, from the slope and intercept of the straight lines.

The entropy of activation was calculated from the equation

$$A = [kT_s/h] \exp(\Delta S/R)$$

where k is the Boltzmann constant, h is Planck's constant and ΔS is the entropy of activation. The heat of reaction ΔH was evaluated from the DTA peak area.

Mechanism of reaction

Deduction of the mechanism of reaction from non-isothermal methods has been discussed by Sestak and Berggren [12]. Kinetic parameters are evaluated from non-isothermal TG–DTA curves by the application of the Arrhenius equation:

$$d(\alpha)/dT = A/\phi \, e^{-E/RT} f(\alpha)$$

The usual kinetic equations not invoking mechanism are mere extensions of the equations pertinent to homogenous kinetics, where it is assumed that $f(\alpha) = (1 - \alpha)^n$. In contrast, mechanism-invoking kinetic equations are based on the assumption that the form of $f(\alpha)$ depends on the reaction mechanism. A series of $f(\alpha)$ forms are proposed [13] and the mechanism is obtained from the one that gives the best representation of the experimental data. In this study the Coats–Redfern method was used for solving the exponential integral. E and A were calculated in each case from the slope and intercept respectively.

RESULTS AND DISCUSSION

Thermal decomposition of $[Cu(en)_2]Cl_2 \cdot H_2O$

The TG and DTG curves of bis(ethylenediamine)copper(II) chloride monohydrate, given in Fig. 1a, show four stages of decomposition. The temperature of inception T_i, temperature of completion T_f, and DTG peak temperature T_s and percentage mass loss for each stage of decomposition are given in Table 2.

From the mass loss data, the complex appears to decompose in four steps:

$$[Cu(en)_2]Cl_2 \cdot H_2O(s) \rightarrow [Cu(en)_2]Cl_2(s) + H_2O(g)$$

$$[Cu(en)_2]Cl_2(s) \rightarrow Cu(en)Cl_2(s) + en(g)$$

$$Cu(en)Cl_2(s) \rightarrow CuCl(s) + en(g) + 1/2Cl_2(g)$$

$$2CuCl(s) \rightarrow Cu(s) + CuCl_2(g)$$

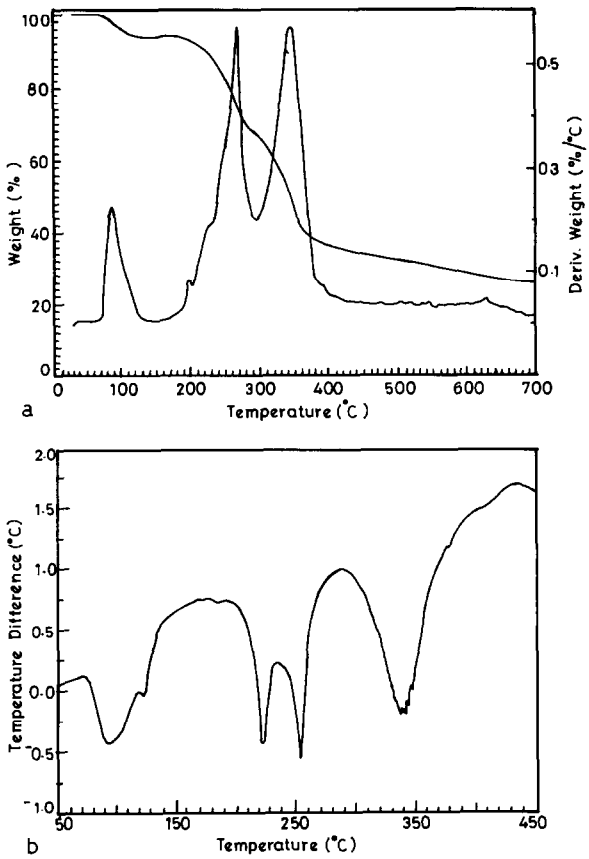

Fig. 1. TG, DTG and DTA curves of $[Cu(en)_2]Cl_2 \cdot H_2O$.

The first stage of mass loss ($T_s = 87°C$) corresponds to the loss of one molecule of water of crystallization of the complex to form the bis(ethylenediamine) complex. This compound could be a square planar product. Usually in bis(ethylenediamine) complexes, the copper(II) ion will occupy an essentially tetragonal environment, with the ethylenediamine ligands coordinating to form an approximately square coplanar structure with the methylene groups of the ligand occupying a gauche configuration. The tetragonal positions are occupied by atoms from the anions. In the chloride and bromide monohydrate the water molecule occupies one tetragonal position, the second being occupied by a halide ion [14,15]. Hence the thermal decomposition is consistent with the crystal structure of the complex. The dehydration stage appears as the first endothermic peak ($T_{max} = 94°C$) in the DTA curve (Fig. 1b).

The second stage involves the deamination of the bis(ethylenediamine) complex to form the intermediate $Cu(en)Cl_2$. This deamination stage in the DTA trace involves two endothermic peaks having $T_{max} = 221°C$ and T_{max}

TABLE 2

Phenomenological data for the thermal decomposition of bis(ethylenediamine)copper(II) halide monohydrate complexes from TG curves

Stage	Decomposition mode	T_i (°C)	T_f (°C)	T_s (°C)	Mass loss (%)	
					Theoretical	Observed
$[Cu(en)_2]Cl_2 \cdot H_2O$						
I	Loss of one H_2O	60	125	87	6.60	6.2
II	Loss of one en	205	280	267	28.63	29.0
III	Loss of one en and one Cl	280	375	348	63.66	63.0
IV	Volatilization of $CuCl_2$	375	770		76.67	75.4
$[Cu(en)_2]Br_2 \cdot H_2O$						
I	Loss of one H_2O	80	105	90	4.98	5.0
II	Loss of one en	200	280	267	21.58	22.6
III	Loss of one en and one Br	280	380	351	60.30	60
IV	Volatilization of $CuBr_2$	380	750		82.41	87.0

= 254 °C respectively. This may be attributed to the time lag involved in the breaking of the two coordinate bonds between the bidentate ligand and the metal. Since copper(II) usually has coordination number four, the mono(ethylenediamine) could be formed by anation of chloride ions with retention of the original square coplanar structure. The formation of the mono(amine) complex has been reported in an earlier publication [6].

The third stage, which follows immediately, involves the mass loss corresponding to the decomposition of mono(ethylenediamine) to form CuCl with the liberation of volatile en and chlorine. In DTA this appears as an endothermic peak with $T_{max} = 340$ °C. The subsequent mass loss (12%) in the TG is a slow process (375–800 °C) probably due to the disproportionation of CuCl into cupric chloride (which volatilizes) and metallic copper. This is shown as continuous drift in DTA.

A comparison of the powder diffractograms with the JCPDS powder diffraction file has shown that the intermediate isolated at 450 °C is predominantly CuCl, whereas the final residue isolated at 700 °C is X-ray pure copper [16]. The X-ray diffraction patterns of the intermediate and the final residues are shown in Fig. 2. The major intensities along with the d spacings are tabulated in Table 3.

The results from DTA curves, namely temperature of inception T_i, temperature of completion of reaction T_f and DTA peak temperature T_{max} for the four endotherms and the enthalpy of transition accompanying them are quoted in Table 4. ΔH for the dehydration process is 42.8 cal g^{-1} and the overall heat of reaction for the second and third endothermic peaks (deamination stage) is 38.0 cal g^{-1}. ΔH for the third stage involves 96.0 cal

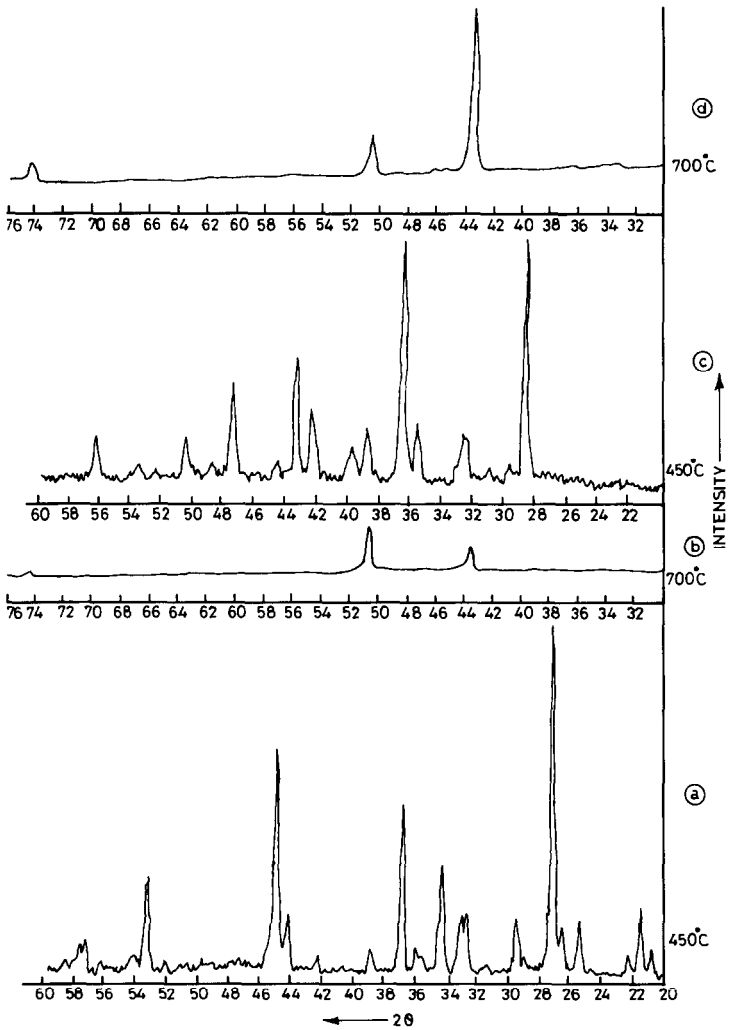

Fig. 2. X-ray powder diffractograms: a and b, $[Cu(en)_2]Cl_2 \cdot H_2O$; c and d, $[Cu(en)_2]Br_2 \cdot H_2O$.

g^{-1}. This higher value is due to the additive effect of both deamination and dechlorination processes occuring simultaneously to give rise to CuCl.

Thermal decomposition of $[Cu(en)_2]Br_2 \cdot H_2O$

From the mass loss, the complex appears to decompose in four stages:

$$[Cu(en)_2]Br_2 \cdot H_2O(s) \rightarrow [Cu(en)_2]Br_2(s) + H_2O(g)$$

$$[Cu(en)_2]Br_2(s) \rightarrow Cu(en)Br_2(s) + en(g)$$

$$[Cu(en)Br_2](s) \rightarrow CuBr(s) + en(g) + 1/2Br_2(g)$$

$$2CuBr(s) \rightarrow Cu(s) + CuBr_2(g)$$

TABLE 3

X-Ray powder diffraction data

$[Cu(en)_2]Cl_2 \cdot H_2O$				$[Cu(en)_2]Br_2 \cdot H_2O$			
450 °C		700 °C		450 °C		700 °C	
d (Å)	I/I_0	d (Å)	I/I_0	d (Å)	I/I_0	d (Å)	I/I_0
3.2572	100.00	1.8038	100.00	3.1104	100.00	2.09	100.00
2.8102	65.93	2.0804	56.52	2.4564	98.44	1.81	46.00
2.4358	49.78	1.2765	4.34	2.0895	51.36	1.28	20.00
2.6202	33.79			1.9194	42.02		
1.7186	29.67			2.1356	31.12		
4.1329	22.25			2.5224	26.77		
2.7466	19.78			2.3243	24.90		
2.7182	19.50			2.7548	23.65		
3.0228	18.95			2.7714	21.01		
2.0464	18.95			1.8105	20.23		
3.4997	18.13			1.6366	20.23		
3.3510	16.48			2.7450	18.67		
2.6999	16.20			2.2702	16.34		
1.6078	12.63			3.0118	10.89		
1.5976	11.81			1.8661	10.11		
4.2949	10.98			1.7157	10.11		
2.4946	10.98			2.0402	10.50		
2.3151	10.71			2.8865	9.33		
3.9864	9.89						
3.0706	9.01						
2.1317	8.24						
1.6922	7.96						
2.5217	7.91						
1.8288	6.86						
1.7529	6.59						
1.5752	6.59						
1.6340	6.04						
2.8506	6.04						
3.6187	4.94						

The first mass loss ($T_s = 90$ °C) corresponds to the loss of one molecule of water to form $[Cu(en)_2]Br_2$ (Fig. 3a). The second stage corresponds to the deamination of bis(ethylenediamine)copper(II) bromide to mono(ethylenediamine)copper(II) bromide. This mono(ethylenediamine) complex may be formed due to an anation reaction as discussed above. As in the $[Cu(en)_2]Cl_2 \cdot H_2O$ decomposition, the third stage corresponds to a mass loss due to the simultaneous liberation of one molecule of ethylenediamine along with the partial evolution of bromine. The partial liberation of these types of moieties has been reported elsewhere [17,18]. This culminates in the formation of CuBr. The subsequent mass loss predominantly involves disproportionation of CuBr into $CuBr_2$ (which volatilizes) and formation of

TABLE 4

Endothermic reaction temperatures and ΔH values for the thermal decomposition of copper(II) halide complexes from DTA curves

Stage	T_i (°C)	T_f (°C)	T_s (°C)	ΔH (cal g^{-1})
$[Cu(en)_2]Cl_2 \cdot H_2O$				
I	74	131	93	42.8
II (i)	191	230	221	17.1
(ii)	234	282	254	20.8
III	290	401	340	96
$[Cu(en)_2]Br_2 \cdot H_2O$				
I	69	144	91	40.2
II (i)	194	236	222	14.0
(ii)	242	285	254	13.8
III	288	420	339	87.2

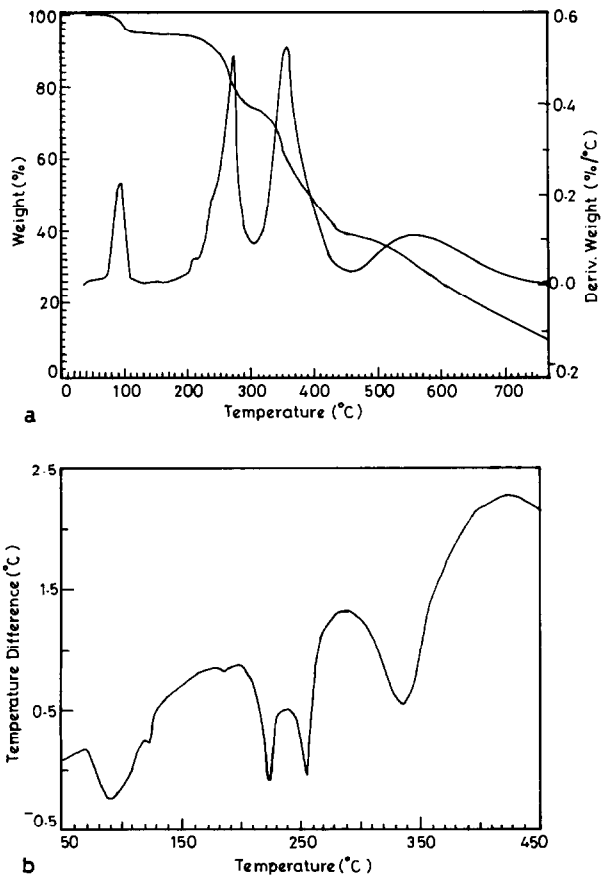

Fig. 3. TG, DTG and DTA curves of $[Cu(en)_2]Br_2 \cdot H_2O$.

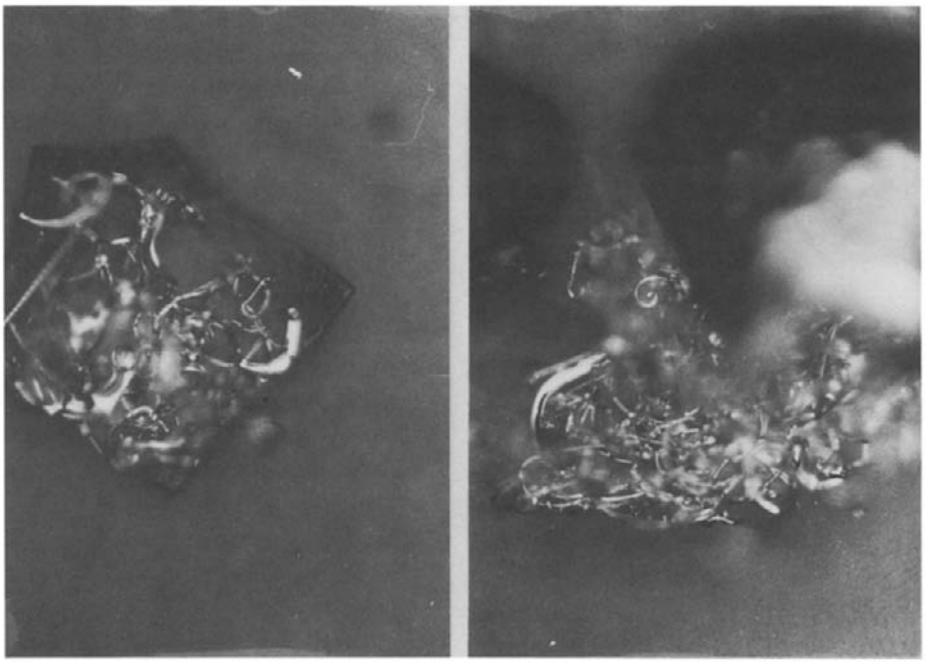

Fig. 4. Microphotographs of residue of $[Cu(en)_2]Br_2 \cdot H_2O$.

metallic copper. This is shown as a continuous drift in DTA. Analogously to the chloride counterpart, the XRD analysis revealed the presence of phases corresponding to different forms of CuBr at this temperature (450 °C). The XRD analysis of the residue at 700 °C confirmed only the presence of copper.

The DTA profile of the complex showed four endothermic peaks (Fig. 3b). The first peak ($T_{max} = 91$ °C) is due to the dehydration process. The second ($T_{max} = 222$ °C) and third ($T_{max} = 254$ °C) endotherms, with almost the same intensity, are due to the disruption of the coordinated bonds as discussed above. The fourth broad endotherm ($T_{max} = 339$ °C) in DTA is due to the reaction depicted by the third stage above. The last stage corresponding to the simultaneous volatilization and decomposition of CuBr to copper appears as a continuous drift as in the case of the chloride complex. In both cases the mass loss recorded is more than that corresponding to the decomposition to metallic copper. Independent pyrolysis at 700 °C in an N_2 atmosphere produced pure copper. This prompted us to presume simultaneous decomposition and volatilization. In both cases the residue at 700 °C viewed through an optical microscope appeared as fine chain-like copper wire of approximate diameter 10–20 μm. Optical microphotographs of the residue of the bromide complex are shown in Fig. 4. Usually such residues are fine powders. In this case the peculiar phenomenon of the formation of fine wire-like structures can be attributed to the

thermal rearrangements taking place in the complex during heating. In order to satisfy the coordination number of copper, the complex may be rearranged and stacked to form a linear polymer with metal–metal bonding and this can decompose to give a linear metallic skeleton as observed under the optical microscope. These types of phenomenon are not uncommon in the coordination chemistry of metals [19].

Kinetics and mechanism

The kinetic parameters were evaluated from TG only for the first two stages of thermal decomposition of bis(ethylenediamine) complexes, since these were the only clear-cut and non-overlapping stages. Using DTA the kinetic analysis was done only for the dehydration step since the subsequent stages are overlapping. Non-mechanistic as well as mechanistic equations were employed. The results from the non-mechanistic equations for chloride and bromide complexes are tabulated in Tables 5 and 6 respectively. The correlation coefficients (r) are in the range 0.9955–0.9994 indicating nearly perfect fits. It can be seen from these tables that the order parameter for the

TABLE 5

Kinetic parameters for the decomposition of $[Cu(en)_2]Cl_2 \cdot H_2O$ using non-mechanistic equations from TG and DTA

Parameter		Equation [a]	Stage I		Stage II
			TG	DTA	TG
n			1.52	1.52	0.52
E	(kJ mol^{-1})	CR	96.20	102.4	114.0
		HM	96.56	102.5	131.0
		MT	94.53	100.9	115.0
		MKN	96.33	102.5	114.3
A	(s^{-1})	CR	9.32×10^{11}	2.98×10^{12}	8.77×10^{8}
		HM	1.00×10^{12}	2.90×10^{12}	4.13×10^{10}
		MT	5.21×10^{11}	1.73×10^{12}	9.65×10^{8}
		MKN	9.71×10^{11}	3.10×10^{12}	9.14×10^{8}
ΔS	(J K mol^{-1})	CR	−17.40	−7.90	−78.65
		HM	−16.81	−8.10	−46.62
		MT	−22.23	−12.40	−77.85
		MKN	−17.06	−7.56	−78.30
r		CR	0.9984	0.9955	0.9975
		HM	0.9983	0.9966	0.9974
		MT	0.9986	0.9960	0.9978
		MKN	0.9984	0.9955	0.9975

[a] CR, Coats–Redfern; HM, Horowitz–Metzger, MT, MacCallum–Tanner, MKN, Madhusudanan–Krishnan–Ninan.

TABLE 6

Kinetic parameters for the decomposition of $[Cu(en)_2]Br \cdot H_2O$ using non-mechanistic equations from TG and DTA

Parameter		Equation [a]	Stage I		Stage II
			TG	DTA	TG
n			1.53	1.53	1.01
E	(kJ mol^{-1})	CR	194.9	118.8	173.1
		HM	199.7	122.0	189.3
		MT	193.8	117.3	174.6
		MKN	194.9	118.9	173.2
A	(s^{-1})	CR	3.10×10^{26}	8.68×10^{14}	7.84×10^{14}
		HM	1.48×10^{27}	2.32×10^{15}	2.98×10^{16}
		MT	2.02×10^{26}	4.80×10^{14}	1.01×10^{15}
		MKN	3.16×10^{26}	9.01×10^{14}	8.13×10^{14}
ΔS	(J K mol^{-1})	CR	260.6	39.40	35.29
		HM	273.6	47.57	65.55
		MT	257.0	34.48	37.41
		MKN	260.7	39.70	35.59
r		CR	0.9994	0.9976	0.9986
		HM	0.9992	0.9977	0.9984
		MT	0.9994	0.9979	0.9988
		MKN	0.9994	0.9976	0.9986

[a] CR, Coats–Redfern; HM, Horowitz–Metzger; MT, MacCallum–Tanner; MKN, Madhusudanan–Krishnan–Ninan.

dehydration and deamination processes is a fraction. It is known from the literature [20,21] that this apparent order n does not necessarily have to be an integer.

The kinetic parameters evaluated by the four equations may be compared. Tables 5 and 6 show that the kinetic parameters computed with the Horowitz–Metzger equation are higher than those from the other three equations. This is due to the inherent error involved in the approximation method employed in the derivation of the Horowitz–Metzger equation. The higher value of E for the bromide complex may be ascribed to the steric hindrance caused by the relatively bulky bromide atom, hindering the easy escape of en and H_2O. In the case of the chloride complex, good agreement of kinetic parameters is obtained between TG and DTA. However, for the bromide complex the agreement is poor. This can be corroborated from the phenomenological data. There is fairly good agreement in the reaction interval ($T_f - T_i$) for TG and DTA (TG, 65; DTA, 58 °C) for the chloride complex. However, for the bromide complex the concordance is poor (TG, 25; DTA, 75 °C). The difference in the value of the reaction interval indicates the difference in the rate of change of reaction rate, a shorter

reaction interval giving rise to a steeper kinetic curve. This results in a higher value of E, which in most cases is offset by a corresponding increase in the A value, attributed to the so-called kinetic compensation effect [22]. The dehydration and deamination processes of bis(ethylenediamine)copper(II) chloride monohydrate have a negative value of entropy, which indicates that for these processes the activated complex has a more ordered structure than the reactant, and the reaction in these cases may be described as "slower than normal". The thermal dehydration and deamination processes of the bis(ethylenediamine) bromide monohydrate have a positive value of entropy,

TABLE 7

Kinetic parameters for the decomposition of $[Cu(en)_2]Cl_2 \cdot H_2O$ using mechanistic equations from TG and DTA

Mechanistic eqn. no.	Form of $g(\alpha)$	Parameter	Stage I		Stage II
			TG	DTA	TG
1	α^2	E	59.91	74.98	201.1
		A	1.14×10^{6}	8.81×10^{7}	2.05×10^{17}
		r	0.94207	0.95334	0.99437
2	$\alpha+(1-\alpha)\ln(1-\alpha)$	E	77.28	92.86	221.7
		A	2.62×10^{8}	2.12×10^{10}	1.58×10^{19}
		r	0.96328	0.97133	0.99708
3	$[1-(1-\alpha)^{1/3}]^2$	E	104.2	119.6	248.4
		A	7.95×10^{11}	4.36×10^{13}	2.31×10^{21}
		r	0.98364	0.98821	0.99728
4	$(1-2/3\alpha)-(1-\alpha)^{2/3}$	E	85.95	101.4	230.5
		A	1.31×10^{9}	9.01×10^{10}	2.95×10^{19}
		r	0.97178	0.97835	0.99756
5	$-\ln(1-\alpha)$	E	64.82	72.13	134.4
		A	1.67×10^{7}	9.98×10^{7}	1.32×10^{11}
		r	0.99326	0.99519	0.99397
6	$[-\ln(1-\alpha)]^{1/2}$	E	29.30	32.89	62.89
		A	7.90×10^{1}	1.97×10^{2}	6.97×10^{3}
		r	0.99163	0.99390	0.99306
7	$[-\ln(1-\alpha)]^{1/3}$	E	17.46	19.81	39.04
		A	1.20×10^{0}	2.21×10^{0}	2.26×10^{1}
		r	0.98902	0.99276	0.99214
8	$1-(1-\alpha)^{1/2}$	E	42.39	50.06	113.3
		A	2.91×10^{3}	2.44×10^{4}	3.62×10^{8}
		r	0.97219	0.97930	0.99743
9	$1-(1-\alpha)^{1/3}$	E	49.02	56.66	119.9
		A	2.09×10^{4}	1.61×10^{5}	1.22×10^{9}
		r	0.98132	0.98665	0.99715

which indicates that for these processes the activated complex has a less-ordered structure than the reactant and the reaction in these cases may be described as "faster than normal" [23].

Choice of reaction mechanism

The values of E and A obtained for the nine mechanistic equations along with the correlation coefficients (r) for the kinetic plots from the TG and DTA data are presented in Tables 7 and 8 respectively. It can be seen that

TABLE 8

Kinetic parameters for the decomposition of $[Cu(en)_2]Br_2 \cdot H_2O$ using mechanistic equations from TG and DTA

Mechanistic eqn. no.	Form of $g(\alpha)$	Parameter	Stage I		Stage II
			TG	DTA	TG
1	α^2	E	182.5	140.8	251.1
		A	9.17×10^{23}	2.53×10^{17}	1.29×10^{22}
		r	0.94613	0.96769	0.98508
2	$\alpha+(1-\alpha)\ln(1-\alpha)$	E	210.7	156.6	278.2
		A	7.77×10^{27}	3.08×10^{19}	4.15×10^{24}
		r	0.96281	0.97839	0.99166
3	$[1-(1-\alpha)^{1/3}]^2$	E	252.2	177.6	314.1
		A	2.61×10^{33}	9.34×10^{21}	4.75×10^{27}
		r	0.98140	0.98883	0.99702
4	$(1-2/3\alpha)-(1-\alpha)^{2/3}$	E	224.0	163.5	289.9
		A	1.68×10^{29}	7.28×10^{19}	1.51×10^{25}
		r	0.96997	0.98246	0.99395
5	$-\ln(1-\alpha)$	E	147.0	97.23	172.5
		A	2.18×10^{19}	4.83×10^{11}	6.74×10^{14}
		r	0.99260	0.99462	0.99867
6	$[-\ln(1-\alpha)]^{1/2}$	E	70.46	45.55	81.85
		A	1.31×10^{8}	1.60×10^{4}	5.50×10^{5}
		r	0.99198	0.99384	0.99853
7	$[-\ln(1-\alpha)]^{1/3}$	E	44.95	28.31	51.63
		A	2.02×10^{4}	4.43×10^{1}	4.37×10^{2}
		r	0.99118	0.99275	0.99829
8	$1-(1-\alpha)^{1/2}$	E	112.8	80.58	143.8
		A	8.02×10^{13}	7.25×10^{8}	3.43×10^{11}
		r	0.97230	0.98320	0.99461
9	$1-(1-\alpha)^{1/3}$	E	123.0	85.73	152.6
		A	1.86×10^{15}	2.92×10^{9}	1.93×10^{12}
		r	0.98051	0.98791	0.99681

the highest values of the correlation coefficients obtained from the two thermal techniques for the dehydration and deamination processes are for the Mampel equation (eqn. (5)).

It can also be seen from Tables 7 and 8 that some other equations give good linear curves with high correlation coefficients, though not as high as eqn. (5). Therefore, it may become difficult to assign the reaction mechanism unequivocally from the linearity of the kinetic curves alone. In such cases the operating mechanism can also be chosen by comparing the kinetic parameters with those obtained by a non-mechanistic equation [24]. In the present case a comparison with the values obtained by the Coats–Redfern method will be more appropriate as the same method was used for solving the exponential integral. From the results given in Tables 5 and 6 it can be seen that the activation parameters calculated for the dehydration and deamination processes using the Coats–Redfern equation are in good agreement with the values obtained from the Mampel equation for both TG and DTA. Thus we can infer that the rate-controlling process for both these reactions are random nucleation with the formation of one nucleus on each particle. The difference in kinetic parameters of the dehydration and deamination processes for both the complexes in no way affects the mechanism of these processes.

ACKNOWLEDGEMENTS

The authors are grateful to the authorities of the Vikram Sarabhai Space centre for providing instrumental facilities. The help of Dr. K. Krishnan and Mr. G. Viswanathan Asari in the TG/DTA instrumental work is gratefully appreciated. One of the authors (S.M.) is grateful to the Council of Scientific and Industrial Research, New Delhi, for giving him a Senior Research Fellowship.

REFERENCES

1 C. De, P.K. Biswas and N.R. Chaudhuri, Bull. Chem. Soc. Jpn., 56 (1983) 3145.
2 J.E. House, Jr., and F.M. Tahir, Thermochim. Acta, 118 (1987) 191.
3 J. Ribas, M. Serra, A. Escuer and H.D. Baro, Thermochim. Acta, 80 (1984) 103–113.
4 J.E. House, K.A. Kemper and H.M. Fogel, Thermochim. Acta, 129 (1988) 263.
5 S. Mathew, C.G.R. Nair and K.N. Ninan, Thermochim. Acta, 144 (1989) 33.
6 C.G.R. Nair, S. Mathew and K.N. Ninan, Thermochim. Acta, 150 (1989) 63.
7 I.M. Procter, B.J. Hathaway and P. Nicholls, J. Chem. Soc. A, (1968) 1678.
8 A.W.Coats and J.P. Redfern, Nature, 201 (1964) 68.
9 J.R. MacCallum and J. Tanner, Eur. Polym. J., 6 (1970) 1033.
10 H.H. Horowitz and G. Metzger, Anal. Chem., 35 (1963) 1464.
11 P.M. Madhusudanan, K. Krishnan and K.N. Ninan, Thermochim. Acta, 97 (1986) 189.

12 J. Sestak and G. Berggren, Thermochim. Acta, 3 (1971) 1.
13 V. Satava, Thermochim. Acta, 2 (1971) 423.
14 F. Mazzi, Rand. Soc. Mineral. Ital., 9 (1953) 148.
15 R.D. Ball, D. Hall, C.E.F. Pickard and T.N. Waters, J. Chem. Soc. A, (1967) 1435.
16 Hannewalt Method Search Manual, International Centre for Diffraction Data, JCPDS, Swarthmore, PA p. 748.
17 J.E. House, Jr. and F.M. Tahir, Thermochim. Acta, 117 (1987) 371–374.
18 J.R. Allan, B.R. Carson, D.L. Gerrard and J. Birnie, Thermochim. Acta, 160 (1990) 329–335.
19 F.A. Cotton and G. Wilkinson, Advanced Inorganic Chemistry, 5th edn., Wiley, New York, 1989, p. 1096.
20 D. Blecic and Z.D. Zivkovic, Thermochim. Acta, 60 (1983) 68.
21 A.C. Norris, M.I. Pope and M. Selwood, Thermochim. Acta, 41 (1980) 357.
22 J.R. MacCallum, Proc. 7th Int. Conf. Thermal Analysis, Ontario, Vol. 1, Wiley, New York 1982, p. 54.
23 J.W. Moore and R.G. Pearson, Kinetics and Mechanism, 3rd edn., Wiley, New York, 1981, p. 181.
24 P.H. Fong and D.T. Chen, Thermochim. Acta, 18 (1977) 273.